Exchange interaction, spin cluster and transport behaviour in perovskites $La_{0.67}Sr_{0.33}(Mn_{1-x}Ni_x)O_3$ ($x \leq 0.2$)

2000 J. Phys.: Condens. Matter 12 601

(http://iopscience.iop.org/0953-8984/12/5/308)

J. Phys.: Condens. Matter **12** (2000) 601–610. Printed in the UK PII: S0953-8984(00)00957-7

Exchange interaction, spin cluster and transport behaviour in perovskites $La_{0.67}Sr_{0.33}(Mn_{1-x}Ni_x)O_3$ ($x \leqslant 0.2$)

Z H Wang†§, J W Cai†, B G Shen†, X Chen‡ and W S Zhan†

† State Key Laboratory of Magnetism, Institute of Physics & Centre for Condensed Matter Physics, Chinese Academy of Sciences, Beijing 100080, People's Republic of China
‡ Department of Physics, University of Science and Technology of China, Hefei, 230026, People's Republic of China

Received 13 January 1999, in final form 4 October 1999

Abstract. A systematic investigation of the magnetic and transport properties of perovskites $La_{0.67}Sr_{0.33}(Mn_{1-x}Ni_x)O_3$ ($x \leqslant 0.2$) is reported. The replacement of the Mn ion by a Ni ion results in a reduction of ferromagnetism and metallic conduction. For the sample with $x = 0.1$, in addition to a metal–insulator (M–I) transition at 240 K, there is a weak insulating behaviour at low temperatures. As the magnetization drop below the Curie temperature (T_C) in the thermomagnetic curve appears for the dosage of $x = 0.15$, the insulating behaviour at low temperatures becomes pronounced. For the sample with $x = 0.2$, a cluster glass-like state with no M–I transition near T_C 194 K is shown. The ferromagnetic superexchange interaction between the $Mn^{3+(4+)}$ ion and the Ni^{2+} ion is found to account for the formation of the cluster glass-like state rather than a spin glass state. All samples have a colossal magnetoresistance (CMR). In particular, with the suppression of the ferromagnetism, the MR effect shifts towards low temperatures and becomes considerably enhanced. Besides the depletion of hopping electrons and the destroyed metallic paths due to the foreign Ni ion terminating the double exchange interaction in the Mn–O network, the randomly frozen spin cluster at low temperatures has been revealed as another crucial factor for localizing charge carriers.

1. Introduction

Increasing interest has been stimulated in perovskite manganites $La_{1-x}A_xMnO_3$ (A = Ca, Sr, Ba, Pb) because of their remarkable magnetic and transport properties [1–4]. The pure compound $LaMnO_3$ is an antiferromagnetic insulator (AFMI) with a Néel temperature of 141 K [5, 6]. When partial replacement of La^{3+} by A^{2+} ions causes the conversion of Mn^{3+} to Mn^{4+}, the double exchange interaction in the Mn^{3+}–O^{2-}–Mn^{4+} bonds drives the oxide to a ferromagnetic metal (FMM) which has a colossal magnetoresistance (CMR) near the metal–insulator (M–I) transition [7, 8]. Interestingly, the CMR effect has been found not only in a conventional FMM system like $La_{0.67}Sr_{0.33}MnO_3$, but also in a FM insulator [9], an AFM charge ordering compound [10] and even spin glass [11, 12]. It is believed that corroborating a detailed relationship between the different magnetic states and the electrical transport is critically important to ascertain the micro-mechanism of the CMR effect. To meet this end, much work in the past few years has centred on structurally tuning the double exchange, usually by doping at a rare earth site. A universal phase diagram trying to predict the possible magnetic and electrical states at a certain tolerance factor and the average ion size at a rare earth site, was first established by Hwang *et al* [13]. In contrast, recent studies have demonstrated

§ Present address: Max-Planck-Institut für Metallforschung, Heisenbergstraße 1, D-70569 Stuttgart, Germany.

0953-8984/00/050601+10$30.00

Table 1. Structural, magnetic and transport parameters of $La_{0.67}Sr_{0.33}(Mn_{1-x}Ni_x)O_3$.

x	a (Å)	α (°)	V (Å^3)	T_C (K)	T_P (K)	M_{S1} (μ_B/f.u.)	M_{S2} (μ_B/f.u.)
0	5.4727	60.38	116.823	365	>300	3.64	3.67
0.10	5.4671	60.39	116.488	289	240	3.34	3.37
0.15	5.4558	60.40	115.965	241	161	3.15	3.22
0.20	5.4538	60.41	115.689	194	—	2.72	3.07

that substitution of Mn with some other element ion could more directly modify the magnetic ordering [12, 14, 15]. Specifically, the transition metal (TM) ion being the foreign ion is of great interest. The reason for this is twofold. First, many TM ions have a perovskite oxide $LaTMO_3$ [16], so single-phase solid solutions are easily obtained. Second, with the magnetic TM ion introduced in the Mn–O network, new magnetic exchange interaction would develop between the TM ion and its neighbouring Mn ion via the 2p state of the oxygen ion. Then, the influence of the magnetic order on transport under these circumstances is no doubt an interesting topic. With these notions in mind, we have performed a preliminary study on the magnetoresistive properties of $La_{0.67}Sr_{0.33}Mn_{0.8}Ni_{0.2}O_3$ [17]. In this paper, we present a systematic investigation of the magnetic and transport properties of the series $La_{0.67}Sr_{0.33}(Mn_{1-x}Ni_x)O_3$. Special attention is focused on the exchange interaction in the Mn–O network, the frozen spin clusters at low temperatures, the electrical transport behaviour, and the interplay between them.

2. Experiment

Ceramic samples $La_{0.67}Sr_{0.33}(Mn_{1-x}Ni_x)O_3$ (LSMNO) with $x = 0$, 0.1, 0.15 and 0.2 were prepared by the conventional solid state reaction method. Detailed synthesizing conditions as well as the crystal structure characterization have been published in a previous paper [17]. The magnetization measurements were carried out on an extracting sample magnetometer (ESM) and a vibrating sample magnetometer (VSM). The resistivity was measured from 1.5 K to ambient temperature by the standard four-probe technique, with the current direction being parallel to the magnetic field direction. In order to check the valence state of the Ni cation in LSMNO, x-ray photoelectron spectra (XPS) of the sample with $x = 0.2$ were accumulated at room temperature on an ESCALAB220I-XL spectrometer with monochromatized Mg Kα x-rays (1253.6 eV) being normal to the sample, and a base pressure of 1.5×10^{-8} Torr.

3. Results and discussion

3.1. Structure and chemistry

Figure 1 shows the x-ray diffraction patterns of the LSMNOs. No impurity or secondary phase, such as La_2NiO_4 type nickelate, was found. The lattice constants a, α and the cell volume V for the rhombohedral unit cell, calculated by the least-squares refinement method, are given in table 1. It is shown that substitution of Ni for Mn does not change the structural symmetry ($R\bar{3}c$) of the parent oxide [18], but leads to a slight decrease in a and V, and an increase in α. Since there is an overlap between the Ni $2p_{3/2}$ peak and the La $3d_{3/2}$ satellite peak in the core-level XPS of the sample with $x = 0.2$, the +2 valence state for the Ni ion in LSMNO is known from a Ni $2p_{1/2}$ binding energy of 871.6 eV, which is almost equal to that of NiO [19]. More recently, by way of EPR (electron paramagnetic resonance) measurement, Rubinstein *et al* also reached a similar conclusion for the valence state of the Ni ion in $La_{2/3}Ca_{1/3}(Mn, Ni)O_3$ [20].

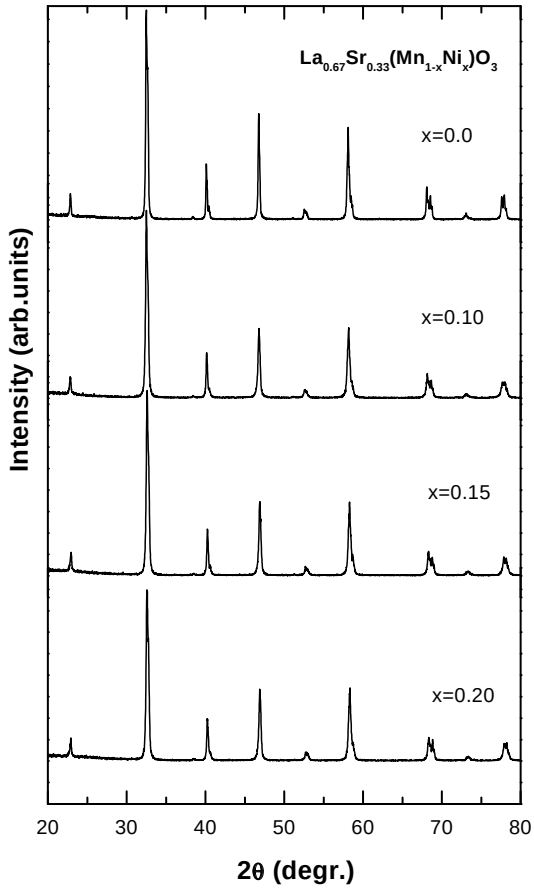

Figure 1. X-ray diffraction patterns of $La_{0.67}Sr_{0.33}(Mn_{1-x}Ni_x)O_3$ ($0 \leqslant x \leqslant 0.2$).

3.2. Magnetic properties

Figure 2 shows the temperature dependence of dc-magnetization (M–T) of the series with $x = 0.1$, 0.15 and 0.2 measured in a field of 500 Oe during the warming process, after being zero field cooled (ZFC) from room temperature to 1.5 K. The inset of this figure shows the temperature dependent ac-susceptibility (χ–T) of the sample with $x = 0$. The Curie temperature T_C values, determined from the maximum point in the $\mathrm{d}M/\mathrm{d}T$ or $\mathrm{d}\chi/\mathrm{d}T$, are listed in table 1. There is a monotonous decrease in T_C with increasing nickel concentration. For the samples with $x = 0$, 0.10 and 0.15, the paramagnetic (PM) state to FM state transition is narrow, however, the transition of the sample with $x = 0.2$ becomes relatively broader. This fact indicates a wider distribution of the magnetic exchange interactions in the Mn–O network. Moreover, for the samples with $x = 0.15$ and 0.2, a magnetization drop appears at certain low temperatures in the M–T curve. Figure 3 shows the M–T curve of the sample with $x = 0.2$ under ZFC and field cooled (FC) runs in a field of 140 Oe. It can be seen that the magnetization drop is related to the size of the measuring field, as reflected by its much lower relative magnitude. Though the FC and ZFC magnetization coincide at high temperatures, even to the broad cusp near T_C, the deviation between them appears just below T_C. All these features are hallmarks of the cluster glass state where the long range FM order is absent [21].

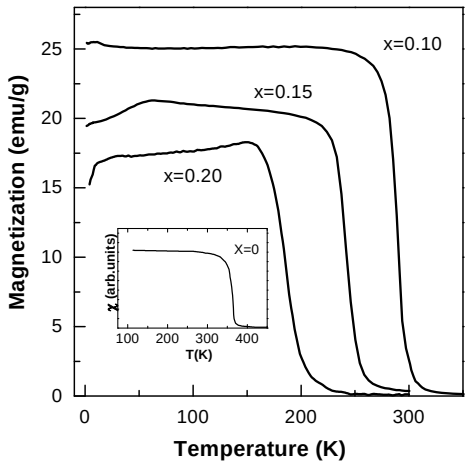

Figure 2. Temperature dependent dc-magnetization of the samples with $x = 0.10$, 0.15 and 0.20 at 500 Oe in ZFC mode. The inset shows the temperature dependence of ac-susceptibility of the sample with $x = 0$.

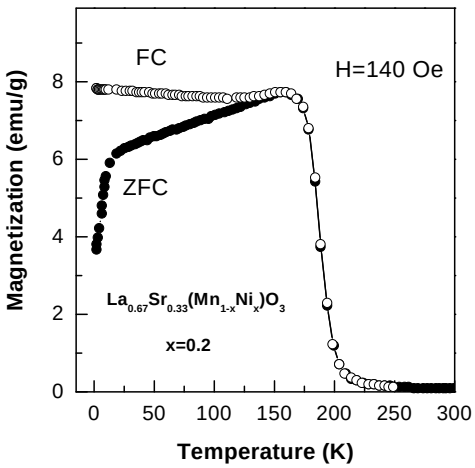

Figure 3. Temperature dependence of dc-magnetization in ZFC and FC runs of the sample with $x = 0.2$ in a field of 140 Oe.

The magnetization isotherms of the LSMNOs taken at 5 K are displayed in figure 4. It can be seen that all samples have the typical FM character. Values for magnetic moment M_{S1} at 65 kOe in Bohr magneton (μ_B) per formula unit (f.u.) for each sample are tabulated in table 1. The magnetization rises at very low field for the samples with $x = 0.15$ and 0.2 which again indicates that their ZFC magnetization drop at low temperatures in the M–T curve should not be attributed to a FM to AFM state transition but a freezing process of spin clusters with FM correlation inside. The small slope of M against H in the high field region for the sample with $x = 0.2$ is related to its cluster glass-like state, while no obvious slope for the sample with $x = 0.15$ suggests a less frozen magnetic moment in this sample at low temperatures. Concerning the FM interaction in the Ni–O–Mn bonds in perovskite La_2NiMnO_6, spinel $ZnNiMnO_4$ and ilmenite $NiMnO_3$ [22], we assume that the magnetic moments of all Mn and Ni ions are aligned in LSMNO, 4 μ_B for $Mn^{3+}(t_{2g}^3 e_g^1)$, 3 μ_B for

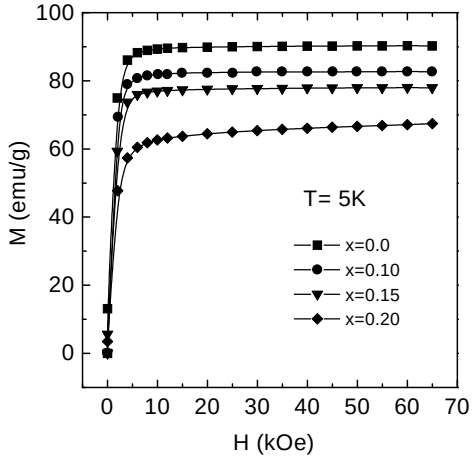

Figure 4. The magnetization isotherms of all samples taken at 5 K.

$Mn^{4+}(t_{2g}^3 e_g^0)$ and 2 μ_B for $Ni^{2+}(t_{2g}^6 e_g^2)$, then the saturation moment M_{S2} of each sample is derived by $M_{S2} = 3.67 - 3x\ \mu_B$/f.u. The calculated values are listed in table 1. The fact that M_{S1} agrees well with M_{S2} lets one argue that the magnetic exchange interaction developing in the Ni^{2+}–O–$Mn^{3+(4+)}$ bonds should be ferromagnetic. Nevertheless, it is also noticeable that the discrepancy between M_{S1} and M_{S2} becomes gradually larger with increasing nickel concentration, implying some spin canting, possibly centering around Ni^{2+}, which exists in the samples with $x = 0.15$ and 0.2 at the high applied field.

Because of the newly joined FM Ni–O–Mn bonds, the overall FM component of LSMNO could still be more than the generic AFM component to the composition with $x = 0.2$. Hence, the FM order persists even when some ratios of the FM double exchange are terminated by the Ni ion. On the other hand, the randomly distributed magnetic exchanges in a contracted lattice reinforce the spin frustration and shorten the FM coherent length, thus, the local freezing process of the FM clusters becomes easy with decreasing temperature.

We note that the analogous spin freezing behaviour at low temperatures has also been observed in several rare earth site doped perovskite manganites, for instance, the compounds at the crossover from FM state to spin glass state in $(La_{1-x}Tb_x)_{2/3}Ca_{1/3}MnO_3$ ($0.04 \leqslant x \leqslant 0.15$) [23], and in other systems like the amorphous Fe_xSn_{1-x} alloy [24]. The spin freezing behaviour in the former case can be ascribed to the bending Mn–O–Mn bond, which increases the magnetic frustration arising from the competition between the AFM interaction and the FM interaction [25]. In the latter case, however, the behaviour is due to the coexistence of direct FM Fe–Fe interaction and indirect AFM Fe–Sn–Fe interaction, which are randomly mixed in the amorphous state [24].

3.3. Zero field resistivity and magnetoresistance

Figure 5 shows the resistivity as a function of temperature (R–T) at zero field and 60 kOe for all samples. Undoped $x = 0$ is metallic in the whole measured temperature region. When the Ni ion is doped in, the M–I transition occurring at a T_P that is lower than the corresponding T_C (see table 1) shifts to low temperature and meanwhile, the resistivity increases accordingly. For $x = 0.2$, the sample has been an insulator at all temperatures. In addition, there are some issues deserving more attention.

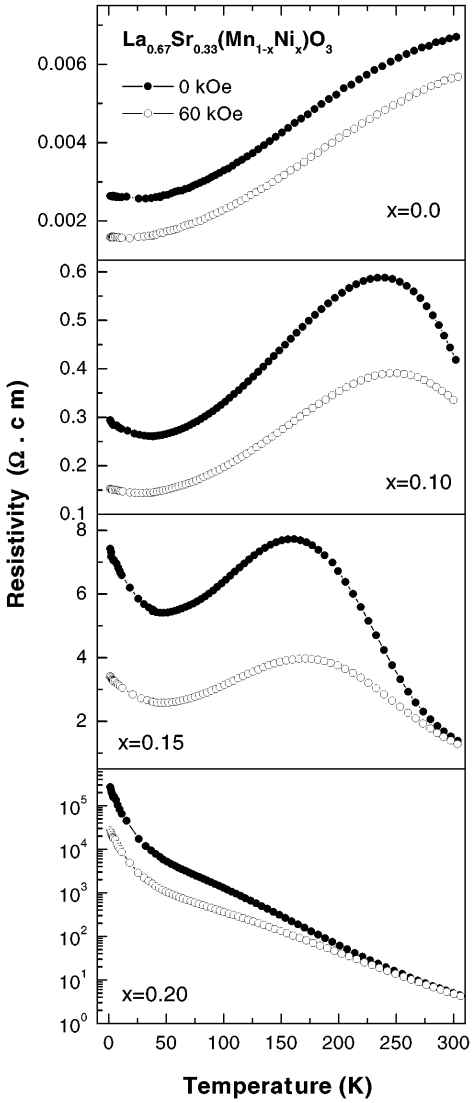

Figure 5. The temperature dependence of the resistivity of all samples at zero field (solid data points) and 60 kOe (open data points).

(a) As double exchange is an interaction mediating both the ferromagnetism and metallic conduction, the decreased M–I transition temperature together with the insulating state of $x = 0.2$ clearly reveal that there should be no charge transfer between the Ni and Mn ions via the O 2p state. The ferromagnetic interaction in the Ni–O–Mn bonds is superexchange rather than double exchange-like, as recently proposed in the Ni–O–Co bonds when the spin glass behaviour and giant magnetoresistance effect in the perovskites $ReCo_{0.7}Ni_{0.3}O_3$ (Re = La, Nd, Sm) were investigated [26].

(b) For the sample with $x = 0.2$, the resistivity above T_C is found to follow the VRH (variable range hopping) law: $\rho \propto \exp(T_0/T)^{1/4}$ [27–29] with $T_0 = 3.65 \times 10^7$ K rather than the activated hopping law: $\rho \propto \exp(E/kT)$. For a clear demonstration, the

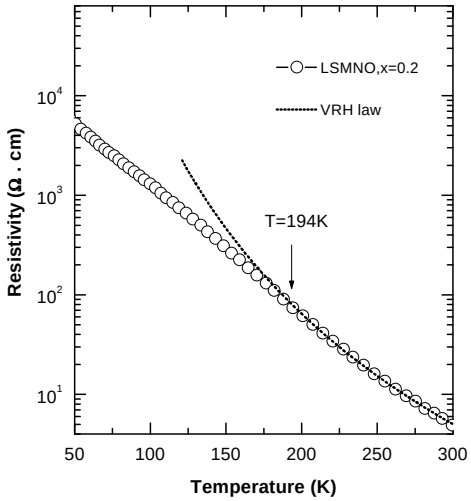

Figure 6. The experimental resistivity and the VRH resistivity at zero field for the sample with $x = 0.2$.

VRH conducting behaviour from 300 K to low temperatures is denoted by the dotted curve in figure 6. It should be mentioned that there are some discrepancies concerning the physical parameters, such as the electron localizing length deduced from T_0 [15], which requires further investigation. However, one can note that the VRH resistivity starts to be larger than the experimental resistivity just at T_C. We believe this fact is important since it shows that the set-in FM order below T_C indeed lowers the kinetic energy needed for electron hopping in the Mn–O–Mn network, which supports the double exchange model [7]. Due to the more and more Ni ions occupying the Mn site, the hopping electrons are depopulated and the metallic Mn–O–Mn network has collapsed when x reaches 0.2. In other words, since the dosage of $x = 0.2$ exceeds the threshold for metallic conduction, we cannot observe a thermally induced M–I transition near T_C.

(c) At low temperatures, the sample with $x = 0.1$ has a weak insulating behaviour. Interestingly, as the low temperature ZFC magnetization drop begins to appear in the sample with $x = 0.15$, the insulating behaviour at low temperatures becomes more pronounced. For the sample with $x = 0.2$, in accord with the ZFC magnetization drop, the resistivity increases drastically below 25 K, showing a different conducting region. Such a tight relationship between magnetism and transport strongly implies that the randomly frozen spin cluster that is detected in the samples with $x = 0.15$ and 0.2, which may be too low to be detected in the sample with $x = 0.1$, is another crucial factor for localizing charge carriers. It is also interesting to note that the localized behaviour associated with the spin freezing process in the aforementioned compounds $(La_{1-x}Tb_x)_{2/3}Ca_{1/3}MnO_3$, is not apparent, in contrast to the behaviour observed here. The reason for this can be explained as follows. For the latter case, due to the replacement of Mn by Ni, the Mn–O network is not perfect. Thus first, the spin clusters may have a smaller size, and in some local region the electron mean free length would be larger than the magnetic coherent length, so additional magnetic scattering occurs. Second, the randomly frozen spin cluster is directly coupled with a fluctuated Coulombic potential from the Mn–O network rather than the rare earth site. As a consequence, the localized state could be more easily introduced in the latter case than in the former case for which the Mn–O network is perfect [27, 30, 31].

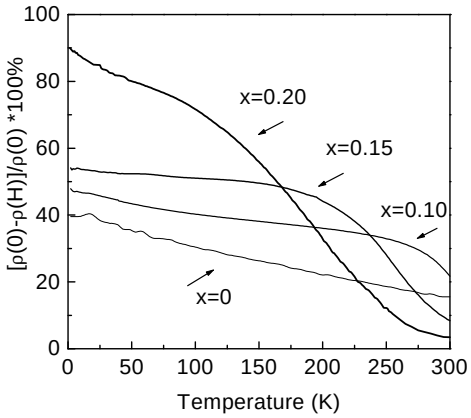

Figure 7. The temperature dependence of the MR ratio of the series at 60 kOe.

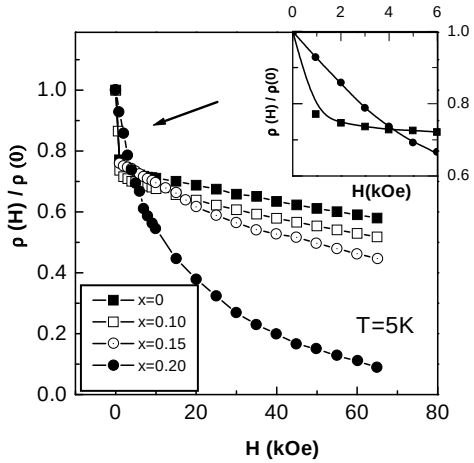

Figure 8. The normalized resistivity as a function of the magnetic field at 5 K. The inset illustrates the low field region of the samples with $x = 0$ and 0.2.

In the applied field of 60 kOe, the M–I transitions move to high temperatures, and the resistivity of all the samples falls significantly. For the samples with $x = 0.1$ and 0.15, the insulating behaviour at low temperatures become weak. For the sample with $x = 0.2$, its low temperature resistivity follows the same trend. Nevertheless, the insulating nature at all temperatures is retained. Figure 7 shows the temperature dependence of the MR ratio, defined here as $\Delta\rho/\rho(0) = [\rho(0) - \rho(H)]/\rho(0)$, where $\rho(0)$ is the resistivity at zero field. One can see that, with decreasing temperature, the MR ratio increases and there is a broad cusp for Ni doped samples near their corresponding T_C. With the suppression of ferromagnetism, the MR effect shows at lower temperatures, but becomes more enhanced compared with the value of the parent oxide $La_{0.67}Sr_{0.33}MnO_3$.

Figure 8 shows the normalized resistivity as a function of magnetic field (ρ–H) up to 65 kOe at 5 K, while the inset illustrates the low field region of the samples with $x = 0$ and 0.2. The compositions with $x \leqslant 0.15$ show two regions in the ρ–H curve. One is the low field region where ρ decreases quite rapidly with H and has a close connection with the

sharp rise in magnetization, as shown in figure 4. The other is the high field region where ρ changes gradually. As for the insulating sample with $x = 0.2$, instead of showing an upturn at low field, the resistivity decreases smoothly, ranging from 0 Oe to 65 kOe, and MR increases extensively, being consistent with the measured temperature dependent MR ratio. Up to now, many of the explorations of the field dependent MR have been undertaken in metallic perovskite manganites and far fewer studies have touched the magnetotransport at given low temperatures in insulating samples. In the present work, the whole magnetic field dependence of MR obtained from metallic $x = 0$ to insulating $x = 0.2$, provides not only an insight into the evolution of the low temperature magnetism, but also a unique opportunity to examine the micro-origin of the enhanced MR at low temperatures with increasing Ni content.

Based on the investigation of MR properties for single crystals and polycrystals, Hwang *et al* pointed out that the low field MR in polycrystalline samples is attributed to the spin polarized intergrain tunnelling (SPIT), and the high field MR arises from the suppression of the intra-grain spin fluctuation [32]. Their argument was later supported by the work led by Mathur *et al* [33]. In our case of ρ–H at 5 K, the SPIT effect is clear for the samples with $x \leqslant 0.15$, and the increasing slope for ρ against H in the high field region, as well as the distinct MR behaviour of the sample with $x = 0.2$, indicates that the series has an increasing intra-grain spin fluctuation. Obviously, such spin fluctuation is not temperature related, which is the case for the metallic samples at higher temperatures, closer to T_C [34, 35], but is spatial and more static. This observation is not surprising since the spin fluctuation is consistent with our suggestion that, with the Mn ion replaced by the Ni ion, the randomly frozen spin clusters grow larger at this low temperature (5 K). With the external field orienting these spin clusters, the magnetic disorder is reduced, which in turn suppresses the spatial spin fluctuation and favours the charge delocalization. We propose that the enhancement of low temperature MR in the series is due to the more enhanced spatial spin fluctuation introduced with increasing Ni content. It is noteworthy that a very similar low temperature MR behaviour, compared with the sample with $x = 0.2$ studied here, has more recently been observed by Ogale *et al* in the epitaxial thin film, with metallic composition $La_{0.67}Ca_{0.33}MnO_3$, where the irradiation of the high energy oxygen ions induced a growth of FM spin clusters [36].

Finally, we would like to note that the applied magnetic field can align the spin but obviously cannot alter the non-perfect nature of the Mn–O network, where randomly distributed Ni ions prevents electron hopping. Therefore, the magnetic field has not induced a M–I transition in the sample with $x = 0.2$. And, due to the unchanged fluctuated Coulombic potential and the residual spin canting which has a memory of the spin freezing process and holds the short magnetic coherent length, the low temperature insulating behaviour is still seen in the samples with $x = 0.15$ and 0.2, even when the magnetic field of 60 kOe is applied, as shown in figure 5.

4. Conclusion

The structure, magnetic and electrical transport behaviour of Ni ion doped $La_{0.67}Sr_{0.33}MnO_3$ have been investigated. Summarizing the experimental results, the following conclusions can be drawn: (a) replacement of Mn by Ni weakens the ferromagnetism and gives rise to the insulating behaviour; (b) randomly distributed superexchange FM Ni–O–Mn bonds are attributed to the appearance of the cluster glass-like state that has a PM to FM phase transition at relatively high temperatures and a spin cluster freezing process at low temperatures, as the Ni content in the Mn–O network increases; (c) besides the depletion of hopping electrons and the destroyed metallic paths owing to the foreign Ni ion terminating the double exchange between Mn^{3+} and Mn^{4+}, the frozen spin cluster at low temperatures is another crucial factor

for the charge localization; (d) the magnetic field reducing the increased magnetic disorder which results in a suppression of the spatial spin fluctuation in the Mn sublattice, is the reason for the considerably enhanced low temperature MR of the series $La_{0.67}Sr_{0.33}(Mn_{1-x}Ni_x)O_3$.

Acknowledgments

This work was supported by the National Natural Science Foundation of China and State Key Project of Fundamental Research of China. We thank T S Ning, J L Wang, N Tang, C P Yang and G D Liu for their experimental help.

References

[1] Jin S, Tiefel T H, McCormack M, Fastnacht R A, Ramesh R and Chen L H 1994 *Science* **264** 413
[2] von Helmolt R, Wecker J, Holzapfel B, Schultz L and Samwer K 1993 *Phys. Rev. Lett.* **71** 2331
[3] Ramirez A P 1997 *J. Phys.: Condens. Matter* **9** 8171
[4] Rao C N R, Mahesh R, Raychaudhuri A K and Mahendiran R 1998 *J. Phys. Chem. Solids* **59** 487
[5] Matsumoto G 1970 *J. Phys. Soc. Japan* **29** 606
[6] Wollan E O and Kochlor W C 1955 *Phys. Rev.* **100** 545
[7] Zener C 1951 *Phys. Rev.* **82** 403
[8] Schiffer P, Ramirez A P, Bao W and Cheong S-W 1995 *Phys. Rev. Lett.* **75** 3336
[9] Argriou D N, Mitchell J F, Potter C D, Hinks D G, Jorgensen J D and Bader S D 1996 *Phys. Rev. Lett.* **76** 3826
[10] Tomioka Y, Asumitsu A, Moritomo Y, Kuwahara H and Tokura Y 1995 *Phys. Rev. Lett.* **74** 5108
[11] Teresa J M D, Ibarra M R, García J, Blasco J, Ritter C, Algarabel P A, Maquina C and Del Moral A 1996 *Phys. Rev. Lett.* **76** 3392
[12] Cai J W, Wang C, Shen B G, Zhao J G and Zhan W S 1997 *Appl. Phys. Lett.* **71** 1727
[13] Hwang H Y, Cheong S-W, Radaelli P G, Marezio M and Batlogg B 1995 *Phys. Rev. Lett.* **75** 91
[14] Ahn K H, Wu X W, Liu K and Chien C L 1996 *Phys. Rev.* B **54** 15 299
[15] Gayathri N, Raychaudhuri A K, Tiwary S K, Gundakaram R, Arulraj A and Rao C N R 1997 *Phys. Rev.* B **56** 1345
[16] Torrance J B, Lacorre P, Asavaroengchai C and Metzger R M 1991 *Physca* C **182** 351
[17] Wang Z H, Shen B G, Tang N, Cai J W, Ji T H, Zhao J G, Zhan W S, Che G C, Dai S Y and Dickon H L Ng 1999 *J. Appl. Phys.* **85** 5399
[18] Urushibara A, Moritomo Y, Arima T, Asamitsu A, Kido G and Tokura Y 1995 *Phys. Rev.* B **51** 14 103
[19] Wagner C D, Riggs W M, Davis L E, Moulder J F and Mouilengber C E (eds) 1979 *Handbook of X-ray Photoelectron Spectroscopy* (Eden Prairie, MN: Perkin Elmer Corporation, Physcial Electronics Division)
[20] Rubinstein M, Gillespie D J, Synder J E and Tritt T M 1998 *Phys. Rev.* B **56** 5412
[21] Mydosh J A 1993 *Spin Glass: An Experimental Introduction* (London: Taylor and Francis)
[22] Blasse G 1965 *J. Phys. Chem. Solids.* **26** 1969
[23] Blasco J, García J, Teresa J M D, Ibarra M R, Algarabel P A and Maquina C 1996 *J. Phys.: Condens. Matter* **8** 7427
[24] Teirlinck D, Piecuch M, Geny J F, Marchal G, Mangin Ph and Janot Chr 1981 *IEEE Trans. Magn.* **17** 3079
[25] García-Muñoz J L, Fontcuberta J, Martínez B, Seffar A, Piñol S and Obradors X 1997 *Phys. Rev.* B **55** R668
[26] Pérez J, García J, Blasco J and Stankiewicz J 1998 *Phys. Rev. Lett.* **80** 2401
[27] Mott N F and Davis E A 1979 *Electronic Processes in Noncrystalline Materials* (Oxford: Clarendon)
[28] von Helmolt R, Wecker J, Samwer K, Haupt L and Barner K 1994 *J. Appl. Phys.* **76** 6925
[29] Fontcuberta J, Martínez B, Seffar A, Piñol S, García-Muñoz J L and Obradors X 1996 *Phys. Rev.* **76B** 1122
[30] Coey J M D, Viret M and Ranno L 1995 *Phys. Rev. Lett.* **75** 3910
[31] Viret M, Ranno L and Coey J M D 1997 *Phys. Rev.* B **55** 8067
[32] Hwang H Y, Cheong S-W, Ong N P and Batlogg B 1995 *Phys. Rev. Lett.* **77** 2041
[33] Mathur N D, Burnell G, Isaac S P, Jackson T J, Teo B-S, MacManus-Driscoll J L, Cohen L F, Evetts J E and Blamire M G 1997 *Nature* **387** 266
[34] Ju H L and Sohn Hyunchul 1997 *Solid State Commun.* **102** 463
[35] Sharma Nirupama, Venkataramani N, Prasad S, Chandra G and Pai S P 1997 *J. Magn. Magn. Mater.* **166** 65
[36] Ogale S B *et al* 1998 *J. Appl. Phys.* **84** 6255